# A Novel Optical Test Bed for Measuring the Light Transmission Properties of Plastic Optical Fiber Under Bending

Eric Huang<sup>1</sup>, Javier Mateo<sup>2</sup>, María Ángeles Losada<sup>2</sup>, Alicia López Lucia<sup>2</sup>, Dayana Ribas<sup>2</sup>, Alfonso Ortega<sup>2</sup>, Eduardo Lleida<sup>2</sup>, Pedro Luis Carro<sup>2</sup>, Dwight Richards<sup>1</sup>, Xin Jiang<sup>1</sup>, Neophytos Antoniades<sup>1</sup>, and Yi Wang<sup>3</sup>

<sup>1</sup>Department of Engineering and Environmental Sciences, CUNY College of Staten Island <sup>2</sup>Aragon Institute for Engineering Research (I3A), University of Zaragoza <sup>3</sup>Electrical and Computer Engineering Department, Manhattan College

Abstract-Plastic optical fibers (POF) possess the potential to occupy a distinctive role in contemporary communication systems, bridging the gap between the attributes of copper cable and glass fiber. POF stands out as a more lightweight and costeffective alternative to glass fiber, while concurrently offering significantly enhanced communication bandwidth compared to traditional copper cables of equivalent cost or weight. However, the novelty of this technology introduces a challenge, as there is limited understanding of how POF cables may behave under specific bending conditions, particularly in the case of the latest multi-core fibers. This paper outlines a research endeavor aimed at establishing a cost-effective and reproducible testing framework for assessing the light transmission properties of plastic optical fibers during various bending conditions. The methodology involves partial automation using National Instruments LabVIEW for servo motor control, and optical power measurements were taken using the Thorlabs PM100USB. The investigation encompassed measurements across diverse bending angles and radii for five distinct types of fibers: Eska MH, Eska BH, Eska GH, a Graded Index fiber, and a Multi Core Fiber.

Index Terms—Plastic Optical Fiber (POF), Step Index (SI), Graded Index (GI), Multi Core (MC), Bending

#### I. Introduction

Optical fibers provide an efficient means of transmitting vast amounts of data over long distances. The introduction of plastic optical fiber (POF) as an alternative to glass fiber and copper cable offers advantages such as higher bandwidth compared to copper, as well as a ruggedness and resistance to mechanical shock that glass cannot provide [1] [2]. The performance of optical fibers is critical to the functionality of communication systems, and one factor that can significantly impact their performance is bending [3] [4]. This research paper explores the effects of bending on 3 main types of POF: Step-index (SI) POF, Graded-index (GI) POF, and Multicore (MC) POF.

All tested fibers were 1-mm poly(methyl methacrylate) (PMMA): three SI-POFs from Mitsubishi: Eska Premier GH4002 (GH) with a numerical aperture (NA) of 0.5, Eska Broadband MH4001 (MH) with NA 0.3, and BH4001 (BH) with 0.6; Optimedia OM-Giga GI-POF (GI), and finally, one 19-core POF from Asahi-Kasei SMCK-1000P (SMCK).

The first part of the paper consists of a thorough description of the bending test-bed, justifying all the features introduced to ensure sound experimental conditions. The novel test-bed is designed to hold tension on a POF while it is being coiled by an optical rotating stage. One end of the POF will be attached to a laser emitter, while the other end will be clamped in place and terminates at an optical power meter, which will measure the optical power throughout its bending cycle. Then, this system is applied to obtain the bending induced signal attenuation of the different types of POF mentioned earlier.

Through an experimental process of investigation, this paper provides a comprehensive overview of the effects of bending on these distinct optical fiber types. The results presented here will contribute to the optimization of optical fiber-based communication systems, ensuring reliable data transmission even in challenging environmental conditions. Additionally, this research may inform the development of novel fiber designs that are more robust against bending-induced losses, further advancing the field of optical communications.

#### II. EXPERIMENTAL DESIGN

# A. Overview

The test-bed is made of 4 distinct parts, each of which serve unique functions. A diagram of the entire test bed and its individual parts is depicted in Figure 1. Figures 2-5 are photographs of each of these four parts.

Firstly, a tension system was constructed in order to provide tension on the POF while it is bent to ensure accurate measurements, as any slack in the POF would cause unpredictable bending behavior. Secondly, a rail system and laser carriage which rides along the rail was constructed. These serve the purpose of allowing the laser emitter to move along a linear track so the tension system is capable of keeping constant tension on the system while it is undergoing its full bending cycle due to the perceived shortening of the fiber as it is bent in an S-curve. Thirdly, there is the bending apparatus itself which performs the bending. This is comprised of a rotating stage with an arm and two spindles mounted on the arm, equidistant from the axis of rotation, around which the POF

will spool. And finally an optical clamp, which serves to hold the POF in place at its terminus so tension can be applied without slippage. All of these parts were bolted down onto two separate optical tables. The output of the POF is attached to a Thorlabs PM100USB optical power meter, connected to a desktop computer and set up to take a measurement every second. All of the 3D printed parts used in this project are printed with Polylactic Acid (PLA).

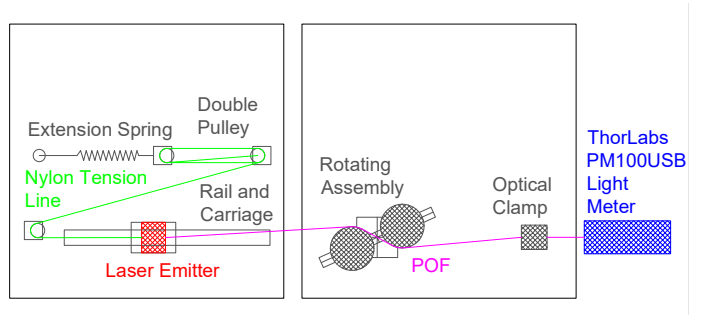


Fig. 1. General Diagram of the Full Test Bed

#### B. Tensioner

Due to the nature of the S-curve induced on the POF changing its overall length, the laser emitter needed to move and be held under tension while undergoing its bending cycles. And so a tension system was constructed using common extension springs, and a compound pulley system using nylon fishing line as a low friction and lightweight tensioning material.

Two double pulleys were made, one fixed and one moving, in order to provide a 4:1 mechanical advantage on the laser emitter so that the spring travel would be minimized in order to allow for a more constant tension to be applied. These parts are shown in Figure 2.



Fig. 2. The double pulley tensioning system

### C. Rail and Laser Carriage Assembly

The rail is comprised of a pair of Newport Optical 26mm rails mounted inline with one another, using dovetail rail carriers to attach it firmly to the optical table, with another pair of rail carriers to attach the laser carrier to the rails. The

laser carrier is made with two composite aluminum boards bolted together. The laser emitter itself is then bolted onto the laser carrier. A pair of 3D printed plastic end caps with springs were made to fit at either end of the rails, in order to protect the laser mount from being damaged by moving past its ends of travel. The rail system and tension pulleys are mounted on the same optical table, as shown in Figure 3.

The composite board laser carriage is designed to mount the LDM9T/M laser diode mount, but it can be modified to accept different mounts as well. The laser emitter installed within the laser mount in this experiment is a L520P50 laser diode with a nominal output power of 50 mW at 520 nm (green), and was polarized using the LDC205C laser controller.

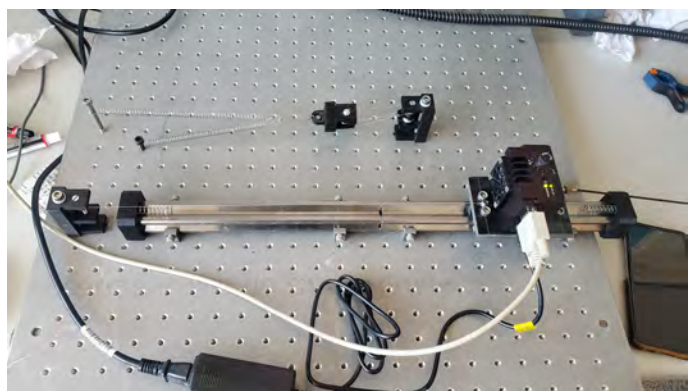


Fig. 3. Laser rail System with tension

# D. Rotating Assembly

The rotating assembly was constructed using a stainless steel bar bolted onto the head of a MicroControle Rotating Stage driven by the MicroControle ITL209 servo controller using a wired GPIB connection to a PC running National Instruments LabVIEW. Two 3D printed spindles are bolted to the steel bar, equidistant from the axis of rotation. These spindles consist of four tiers, with each tier providing a different bending radius. From largest to smallest, the bending radii are: 35mm, 25mm, 15mm, and 7.5mm. Each tier of the spindle is modeled with a v-groove to improve POF retention in the system as it is spooling and unspooling. The rotating assembly is shown in Figure 4.

#### E. Optical Clamp

The optical clamp is necessary for ensuring that the POF is held under tension without slipping by clamping it in place at the terminus. This part consists of a housing, and two half cylinders within the housing that can be pressed up against one another by tightening two pairs of M4 screws located on the outside of the housing. This part is shown in Figure 5.

#### F. NI LabVIEW Virtual Instrument

The current LabVIEW Virtual Instrument used to drive the rotating stage is very simple and is able to run user inputted commands manually as well as run pre-written programs using a case structure. Currently, the only program that has been



Fig. 4. Rotating Assembly

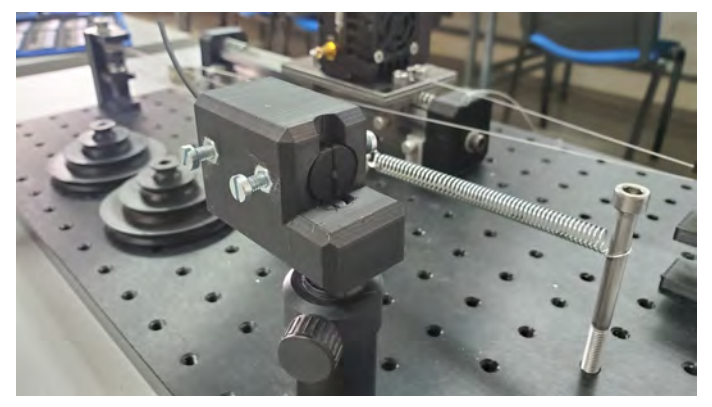


Fig. 5. Optical Clamp

written is a program to drive the motor at 1 degree per second from 0 degrees to 180 degrees and back to 0 degrees, a total of 3 times. In the future, this script can be improved by adding additional capabilities such as the introduction of more bending cycles, or keeping the POF bent over greater periods of time.

# III. RESULTS

Here, we present an application of the proposed POF bending test bed. The transmitted power was monitored while the tested fiber was bent. Output power was measured in decibel-milliwatts (dBm) once every second, while the rotating assembly rotates one degree every second, so that each recorded data point for output power can easily be plotted against a corresponding bending angle. Figure 6 shows the optical power measured with the Eska MH fiber over three bending cycles as a function of time. The axis on the right side of the plot refers to bending angle, and only applies to the green series labeled "Angle." The other series refer to the left side axis, which measures optical power in dBm. The four other series each represent a different bending radius. These same four series as well as their color coding are consistent for each successive graph. The blue lines represent a 35mm radius of bending, the orange lines represent a 25mm radius of bending, the gray lines represent a 15mm radius of bending, and the yellow lines represent a 7.5mm radius

of bending. From Figure 6, it can be shown that the power drops at a certain rate as the bending angle increases, and then increases at a much greater rate once the bending passes 180 degrees. This is most obvious with the gray and orange series in Figure 6, where it can be shown that they seem to asymptotically approach a lower limit as the time approaches 180 seconds, and then rapidly spike back up to a higher value as the bending angle begins to decrease again. This same behavior occurs at 540 seconds and 900 seconds as well, which are the two other instances that the rotating stage reverses direction direction from positive to negative. This behavior is indicative of a hysteresis loop, which can also be found in stress-strain curves of many materials undergoing cyclic stress loading. This characteristic loop is even better illustrated in the following figures.

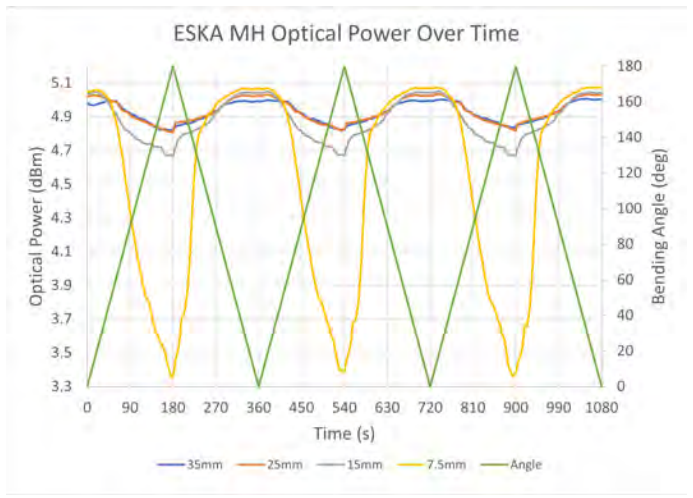


Fig. 6. Measured Power Output of MH POF plotted against time and angle

Figures 7 through 11 show the attenuation of each tested fiber over 3 bending cycles, plotted over bending angle. The attenuation was calculated by selecting the first measured output power of any given fiber at any given bending radius P(0), and then subtracting that from each successive optical power from the same run P(angle), according to the equation below. This effectively eliminates the inconsistency of trying to compare different runs with different initial optical power levels.

Attenuation(fiber, radius) = 
$$P(\text{angle}) - P(0)$$
 (1)

It can be seen that most of the fibers perform fairly well for most bending radii until 7.5mm, where the output power degrades dramatically, especially for the GI POF. Eska MH seems to behave very well throughout the bending cycles, maintaining strong output power throughout the 35mm, 25mm, and 15mm bending radii. However, it experiences an attenuation of -1.7dB when a 7.5mm radius of bending is applied, as seen in Figure 7. Its superior performance compared to the rest of the single core POFs may be attributed to its lower numerical aperture of 0.3 and its double clad design.

Compared to ESKA MH, ESKA GH shows poorer results in Figure 8, decreasing by -4 dB when a 7.5mm bending radius is applied.

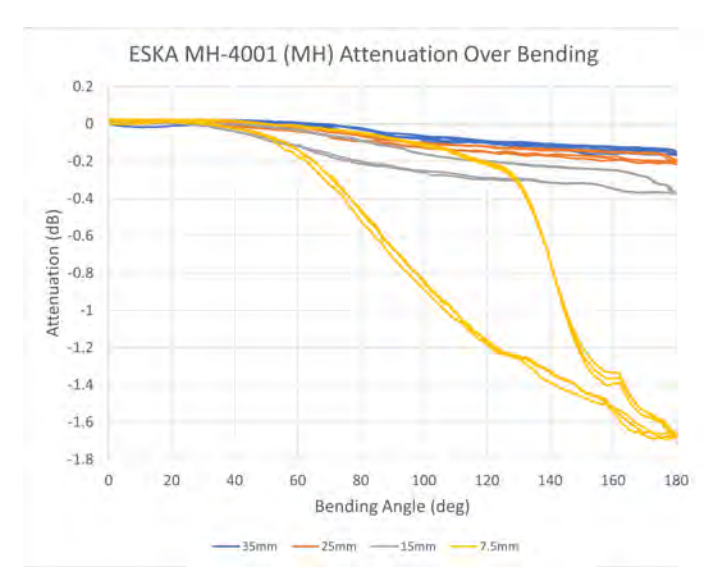


Fig. 7. Calculated attenuation of MH POF plotted against angle

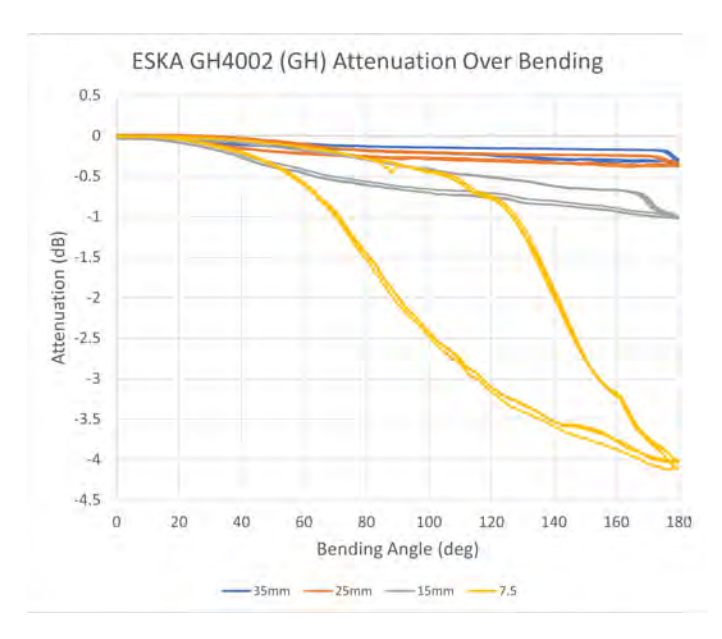


Fig. 8. Calculated attenuation of GH POF plotted against angle

It is important to note that ESKA BH fiber, which is an industrial high temperature POF designed to withstand temperatures of up to 105 degrees Celsius, was much stiffer than the others and required a higher spring tension to attain repeatable results. Also note that the results in Figure 9 reveal that the ESKA BH fiber has a rather poor consistency and overlap between the three bending cycles at any given bending radius. This clearly shows a permanent optical degradation with each bending cycle, despite its favorable overall performance compared to GH, attenuating by only -1.7 dB at 7.5mm. It supports the fact that since BH is made of a stiffer,

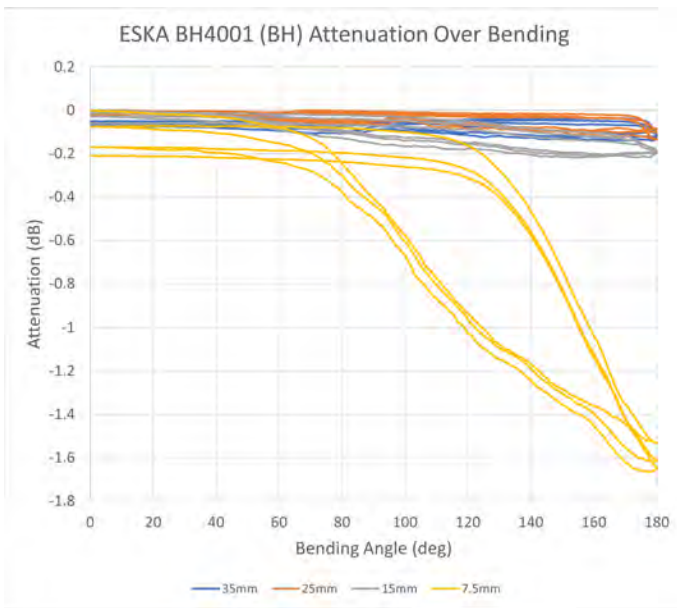


Fig. 9. Calculated attenuation of BH POF plotted against angle

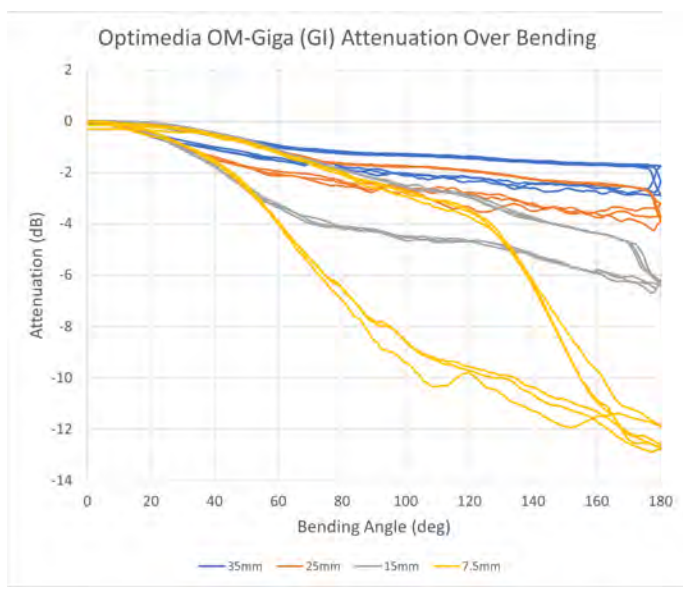


Fig. 10. Calculated attenuation of GI POF plotted against angle

less malleable plastic compound, it is much more prone to optical degradation due to bending [5]. This degradation is exacerbated with repeated bending cycles, making it poorly suited to dynamic situations in which the fiber must undergo repeated bending. It is unclear at the moment if there is a fatigue limit to the optical clarity of POFs, in the same way there is a fatigue limit to the yield stress of certain materials under cyclic loading. This parameter can be tested using this same test-bed in the future.

The GI POF shows the poorest bending performance of the five POFs tested, attenuating by -13dB when subjected to the 7.5mm bending radius.

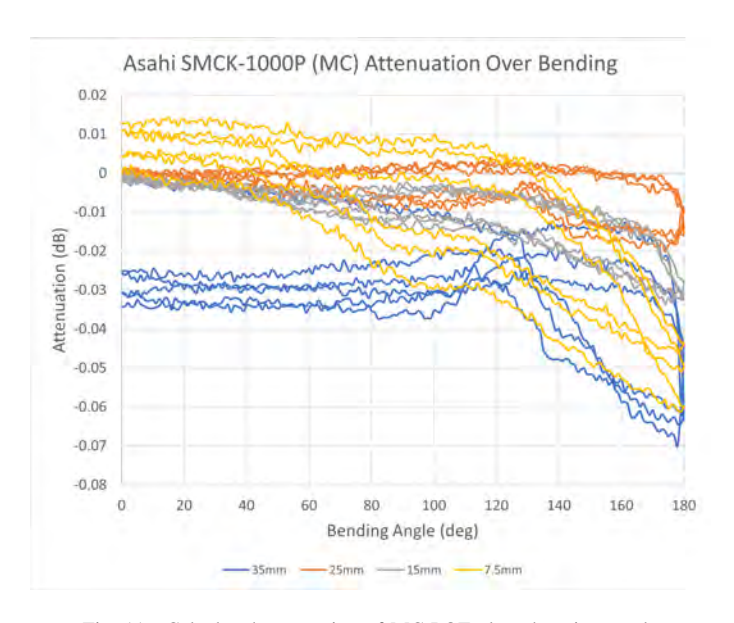


Fig. 11. Calculated attenuation of MC POF plotted against angle

We can also see the phenomenal resistance to bending losses of multi core fiber in this experiment, shown by the results in Figure 11 (notice the significant difference in the scaling of the vertical axis relative to the other figures). Even when put under a 7.5mm bending radius, the signal strength only appears to attenuate by -0.07 dB. In fact, the bending losses are so minimal that random fluctuations in optical intensity can be observed in the graph, meaning the results are approaching the limits of precision that the PM100USB power meter is capable of measuring. This result confirms the incredible resistance that multi core POFs have against bending losses [6].

Additionally, the 35mm series in Figure 11 appears to start at -0.03 dB of attenuation, but it is misleading. The first bending cycle of that series actually begins at 0 dB, but is partially obscured by the other series. Each subsequent bending cycle of the 35mm run show a permanent attenuation of -0.03 dB, even after straightening out the POF. This means the SMCK POF experienced slight permanent optical damage, that only occurs at the first instance of bending, but not the subsequent instances of bending. This same behavior cannot be observed in the 25mm and 15mm series, as its attenuation remains more consistent going forward. However, when put under 7.5mm of bending, the fiber shows a more puzzling behavior. The yellow series in Figure 11 ends at positive values, indicating that the measured power increased after each bending cycle, resulting in an increase of 0.01 dB compared to the beginning of the run. This is opposite to the behavior shown by the BH fiber in the yellow series of Figure 9, which shows worsening attenuation after each run. This may be explained by the very low overall attenuation of this fiber, as well as the higher variability and complexity due to its numerous cores.

## IV. CONCLUSIONS

This experimental system represents an efficient tool to analyze the effects of bending over different transmission properties. Its most attractive characteristic is that it allows us to monitor a parameter (optical power, for example) while the fiber is being bent. Moreover, the set-up has been designed to keep the fiber straight and tense during the whole process, avoiding spurious and unpredictable curvatures. This allows the device to create highly accurate and reproducible results. Also, its design is modular in nature, which provides a flexibility for altering a variety of bending parameters. For example, the bending radius, the angle of bending, the rate of bending, and the number of bending cycles can all be changed with very minor and rapid alterations to the system.

The existence of the test-bed opens up many more future avenues of research into the effects of bending on the signal quality of POFs, which could lead to clearer methods of optimizing the commercial, industrial, or scientific applications of POFs in real word data transmission applications. This could involve recording the bit error rate caused by bending, or measuring the physical degradation of the fiber over repeated bending cycles or holding the fiber under a severe bend angle or radius for an extended duration of time. All of this could be done with a few modifications to the virtual instrument and physical test bed, and would allow for many more insights to be drawn, now that the test bed has been proven to provide repeatable results.

#### V. ACKNOWLEDGMENT

This work was supported by the National Science Foundation Program Standard Grants #2153667, #2153668, under the International Research Experiences for Students (IRES), by the Government of Aragon (T20-23R, T31-23R and T36-23R), by MCIN/AEI/10.13039/501100011033 and the European Union "NextGenerationEU"/PRTR, under grant numbers: PID2021-1260610B-C44, PID2021-1225050B-C33 and PDC2021-120846-C4, and by the European Union's Horizon 2020 research and innovation programme under Marie Skłodowska-Curie Grant 101007666.

# REFERENCES

- O. Ziemann, J. Krauser, P. E. Zamzow, and W. Daum, POF handbook, 2nd ed.; Springer: Berlin/Heidelberg, Germany, 2008.
- [2] C. A. Bunge, T. Gries, and M. Beckers, Eds. Polymer Optical Fibres Fibre Types, Materials, Fabrication, Characterisation and Applications, 1st ed.; Amsterdam, The Netherlands: Elsevier, 2017.
- [3] Gaizka Durana, Joseba Zubia, Jon Arrue, Gotzon Aldabaldetreku, and Javier Mateo, "Dependence of bending losses on cladding thickness in plastic optical fibers," Appl. Opt. 42, 997-1002 (2003)
- [4] M.A. Losada, A. López and J. Mateo, Attenuation and diffusion produced by small-radius curvatures in POFs, Opt. Express 24, 15710-15720 (2016)
- [5] J. Guerrero, M. Angeles Losada, Alicia Lopez, Javier Mateo, Dwight Richards, N. Antoniades, Xin Jiang and Nicholas Madamopoulos "Novel Measurement-Based Efficient Computational Approach to Modeling Optical Power Transmission in Step-Index Polymer Optical Fiber", Photonics, VOL. 9, Issue 4, April 2022
- [6] López Alicia, Ramon Sergio, Chueca Manuel, Losada M. A., Dominguez-Chapman Frank, Mateo Javier. (2016). Experimental characterization of transmission properties in multi-core plastic optical fibers. 1-4. 10.1109/ICTON.2016.7550339.